IEEE Access
Multidisciplinary : Rapid Review : Open Access Journal

Received 29 April 2024, accepted 9 May 2024, date of publication 15 May 2024, date of current version 30 May 2024.

Digital Object Identifier 10.1109/ACCESS.2024.3401091

RESEARCH ARTICLE

Atmospheric Visibility and Cloud Ceiling Predictions With Hybrid IIS-LSTM Integrated Model: Case Studies for Fiji's Aviation Industry

SHIVEEL RAJ[1], RAVINESH C. DEO[1], (Senior Member, IEEE), EKTA SHARMA[1], RAMENDRA PRASAD[2], TOAN DINH[3], AND SANCHO SALCEDO-SANZ[1,4]

[1]School of Mathematics, Physics and Computing, University of Southern Queensland, Toowoomba, QLD 4350, Australia
[2]Department of Science, School of Science and Technology, The University of Fiji, Lautoka, Fiji
[3]School of Engineering, Centre for Future Materials, University of Southern Queensland, Springfield Campus, Springfield Central, QLD 4300, Australia
[4]Department of Signal Processing and Communications, Universidad de Alcalá, Alcalá de Henares, 28805 Madrid, Spain

Corresponding authors: Ravinesh C. Deo (ravinesh.deo@unisq.edu.au) and Shiveel Raj (shiveelraj@gmail.com)

This work was supported in part by Australian Federal Government's Department of Foreign Affairs and Trade through Australia Awards Scholarship Scheme for Fiji, from 2022 to 2024, under Grant 2022; and in part by the Agencia Española de Investigación, Spain, under Grant PID2020-115454GB-C21.

ABSTRACT Atmospheric visibility and cloud ceiling forecasts are essential for the safety and efficiency of flight operations and the aviation industry. Routine hourly aviation meteorological observations are recorded at every airport. However, forecasts of these two meteorological parameters using artificial intelligence techniques are limited. This research utilizes data from two study sites in Fiji, Nadi, and Nausori International Airport, and proposes a hybrid Iterative Input Selection – Long Short-Term Memory (IIS-LSTM) integrated model to forecast the consecutive hour's visibility and ceiling parameters. The IIS algorithm acts as a feature selector from the global predictor matrix of predictor variables with its significant lagged inputs and the significant lagged inputs of the target variable, while the LSTM algorithm acts as the learning model and makes forecasts. The performance of the proposed hybrid IIS-LSTM model is evaluated using seven statistical score metrics and compared with four competing benchmark models. The evaluated results illustrate the superiority of the proposed hybrid IIS-LSTM integrated model and its advanced capability to generate accurate atmospheric visibility and cloud ceiling forecasts for the next consecutive hour compared to the benchmark models. The most important features selected were the second lagged input of visibility and first lagged input of rainfall to improve visibility forecasts while the first and the fifth lagged inputs of the total low cloud cover were paramount for accurate cloud ceiling forecasts. Considering the geography of the study sites, the overall efficacy of the IIS method is strongly advocated to screen most suitable model predictors and the subsequent integration of this input selection method with the LSTM predictive algorithm to attain enhanced performance of the hybrid IIS-LSTM forecast model. This objective model is therefore proposed to be an efficient and cost-effective predictive tool for atmospheric visibility and cloud ceiling forecasts, especially its applications in the aviation industry for aeronautical purposes.

INDEX TERMS Visibility forecast, ceiling forecast, deep learning, machine learning, iterative input selection, long short-term memory.

I. INTRODUCTION

The aviation industry heavily relies on meteorological parameters for the overall safety and efficiency of flight operations in terms of the planning, decision-making and

The associate editor coordinating the review of this manuscript and approving it for publication was Rosario Pecora.

contingency procedures. While all meteorological parameters have their relative importance to the overall aviation operations, of immediate interest are the atmospheric visibility and the low cloud ceiling parameters used at the respective airports for the monitoring of flight safety.

According to the International Civil Aviation Association [1], *visibility*, used as the first objective variable in this research study, is the distance in the lower atmosphere a black object can be seen and identified against a bright background at the ground level, or the distance at which light of 1000 candela in luminescence can be seen and recognized against an unlit background, whichever is greater. The description of *ceiling*, used as the second objective variable in this research study, is the vertical distance of the base of the lowest layer of cloud below 6000m from the surface of the earth or water and which covers more than fifty per cent of the sky [2]. These two variables play a crucial role in the operation of flights, especially in the critical phase of landing and taking-off, since most meteorological-related aircraft incidents occur during periods of poor visibility and low cloud ceiling [3]. Prior studies showed that low clouds and obscuration contributed to about 70% of fatal accidents in general aviation flights [4]. This emphasizes that a timely, reliable, and precise observation of these two meteorological parameters is essential for planning and assisting aircraft in maneuvering through hazardous situations, which is crucial for safe aviation operations.

There are currently products that are operationally implemented providing forecasts of weather elements, including visibility and ceiling, using meteorological reports. For example, in the United States of America, the Gridded Localized Aviation Model Output Statistics Program (GLMP) is implemented which has a 2.5 km horizontal resolution and produces an analysis every 15 minutes. This algorithm extends the Localized Aviation Model Output Statistics Program (LAMP), which is station-based ceiling and visibility analysis produced by the integration of METAR (aerodrome routine meteorological report) and buoy reports (NOAA, 2019). Other products include the National Ceiling and Visibility Analysis (NCVA), the Real-Time Mesoscale Analysis (RTMA) and the Real-Time Mesoscale Analysis Rapid Updates (RTMA-RU). Various types of data are used as inputs into these products including surface observations from a combination of human and automated systems (METAR), fully automated surface observation stations (ASOS), regional networks of automated meteorological observing systems (Mesonets), and satellite data from GOES-16. Despite these products developed for visibility and ceiling analysis, accurate predictive models utilizing meteorological datasets currently remain relatively limited.

The inherent abrupt and stochastic nature of the meteorological system makes mathematical modelling highly complex and resource-intensive [6]. To develop in-situ models with higher frequency and accuracy to make reliable meteorological forecasts of variables such as visibility and ceiling, Artificial intelligence (AI) models and big data approaches are necessary especially in the current era of increasing volume of datasets regarding atmospheric properties recorded at various airports. Scholars have modelled visibility as a classification problem, grading the classes as high, medium, and low or fog versus no fog instances [7], [8], [9]. For instance, a study done at Spain's Valladolid airport used hybrid prediction models such as Proportional Odds Model and Support Vector Machines (SVM) for ordinal classification of visibility events in three categories (FOG, MIST, CLEAR) [10]. Another research tried to forecast hourly short-term low visibility events at the same airport using a combination of Machine Learning (ML) techniques [11]. Similarly, an exploratory study conducted in Florida, USA used various ML algorithms to classify visibility as low, moderate, and good using local weather station data [12].

However, visibility and ceiling forecasts as a regression problem have been least explored and have recently gained some popularity. In a study conducted at Santos Dumont Airport Brazil, four machine learning models were used for both classification and regression forecasting of visibility, and regression forecasting for ceiling base height [13]. Similarly, a low visibility event forecasting study was carried out as both a classification and regression problem in Galicia, Spain using a large number of ML approaches [14]. The authors found the Artificial Neural Network (ANN) model with a simple standardization method to be the most efficient formulation after evaluating the performance of the models under a common framework. Additionally, single-step visibility forecasts using five different deep learning models were studied by [15] for weather stations in Florida. The authors recommended deep learning models for further research in visibility forecasting as a regression problem considering its importance to safety in transportation systems and a lack of similar studies. Furthermore, a study by Pelaez-Rodriguez et. al [16] concluded that a deep learning ensemble methodology gave very satisfactory results in forecasting visibility at two locations in Spain due to the ensemble containing information from all individual learners of the different deep learning architectures.

An essential aspect of model development is model parsimony, i.e., a reduction of overall model input variables whilst achieving the same level of accuracy. This is achieved by discarding irrelevant or redundant variables while selecting only the most applicable variables. The implication is that necessary information is still retained in the dataset, while variables that do not contribute to output information are excluded. The benefits of reducing the dimensionality of the data include a decrease in computational cost, improvement in generalization capability, and reduction in the probability of missing data and outliers being included in the data [17]. These input selection or dimensionality reduction methods can be classified broadly into feature extraction or feature selection techniques. Feature extraction methods transform or combine original inputs to create new features, while feature selection methods use the original input features and select the best subset of features from these.

Feature selection methods are further classified as filters, wrappers, embedded or hybrid [17], [18]. Some filter methods applied in the literature include correlation analysis [19], [20], [21], information-theoretic subset selection (ITTS) [22], minimum Redundancy Maximum Relevancy [23], [24], and the Lipschitz quotient [25] which is a backward elimination filter method. The least absolute shrinkage and selection operator – multilayer perceptron (LASSO-MLP) is an example of an embedded method [26] while studies by [26] and [27] are examples of hybrid methods of feature selection used in literature.

An alternative feature selection method called Iterative Input Selection (IIS) was proposed by [28], which can determine the optimum predictor variables from a global pool using a tree-based algorithm. The accuracy of this algorithm was demonstrated in the study for streamflow forecasting in Ticino River, Switzerland. A further study in [29] revealed that the IIS algorithm performed better than partial mutual information, partial correlation and Genetic Algorithm-ANN. Additionally, the IIS-optimized models have been found to perform better than standalone models in forecasting monthly streamflow in Australia's Murray-Darling Basin and were recommended as a suitable tool for feature selection [31]. Nonetheless, the application of the IIS algorithm in visibility and ceiling forecasting using aviation meteorological observational data is yet to be explored.

Therefore, this study aims to extend the investigative approach of utilizing deep learning architecture AI models for visibility and ceiling forecasting using hourly routine aviation meteorological observation data. The site locations chosen are two international airports in Fiji. To the best of the authors' knowledge, no such research has been undertaken to explore the capabilities of AI models for forecasting the weather elements' visibility and cloud ceiling for these two study sites, let alone deep learning models. Additionally, current literature shows a lack of research being conducted in forecasting visibility and ceiling as regression problems using aviation meteorological observational data.

This study aims to address these gaps in research by advancing the applications of deep learning AI models for visibility and ceiling forecasts, with the following objectives:

1. *Use the Iterative Input Selection (IIS) feature selection technique to find the optimum features for the model from all meteorological variables and significant lagged series.*

2. *Design and implement the proposed hybrid IIS-LSTM integrated model for a 1-hour forecast horizon and compare the outcomes with alternative AI models LSTM, TabNet, ANN and Random Forest.*

3. *Evaluate the performance of the objective model (proposed hybrid IIS-LSTM) with the alternative models using performance evaluation metrics and graphical analysis of the observed dataset with the forecasted dataset.*

4. *Briefly elaborate on the suitability of the objective model for practical visibility and ceiling forecasts, discuss any limitations and comment on any recommendation for future research.*

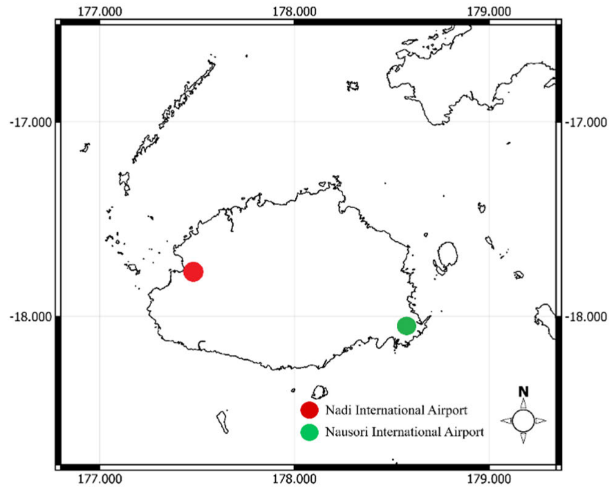

FIGURE 1. Map of Fiji showing the present study locations for which the proposed IIS-LSTM model was developed and implemented.

II. THEORETICAL OVERVIEW

A. ITERATIVE INPUT SELECTION (IIS) ALGORITHM

The study of [28] has proposed the IIS as a robust input selection tool that utilizes highly randomized trees (Extra trees). The IIS is not computationally intensive; thus, faster, and more efficient [32]. The IIS algorithm is executed in three phases. The first phase is the Input Ranking (IR), whereby the most significant predictors are selected in a forward selection method process. The variables are ranked in order or significance, but the contribution of each input information towards the output may be hidden due to the possibly redundant variable(s).

Therefore, the second phase groups the most significant p-ranked variables and assesses their significance using a Single Input Single Output (SISO) approach. The Extra-Trees model with the SISO approach is trained and compared to the observed outputs and assessed based on accuracy evaluation metrics. Based on this assessment, the best-performing inputs are added to the set p'. The third phase is the Multiple Input Single Output (MISO) phase whereby the prescribed screening model aims to rate the effectiveness of each input matrix in forecasting the output. This is done to minimize overfitting, and the procedure is repeated with the residuals from the previous iteration as the new output variable in the previous 2 phases. The operation is iterated until either the best IR variable is found in the selected p' variables, or the performance of the model does not show significant improvement based on the coefficient of determination (R^2) [33].

To further improve the feature selection process, the IIS algorithm performs K-fold cross-validation, which has the advantage of using all the data in both training and validation, which reduces the possibility of overfitting the model.

B. LONG SHORT-TERM MEMORY (LSTM)

The proposed model is a hybrid, integrating the IIS algorithm with the Long Short-Term Memory (LSTM) architecture. The deep learning LSTM Network model is a special type of Recurrent Neural Network (RNN) which can learn long-term dependencies and therefore can perform well in time-series data predictions [34]. It has memory capabilities because its gate structure is different from the RNN structure and is therefore able to retain historical information for a long time [35], [36]. The technical details of the objective model LSTM architecture are well studied and found in literature elsewhere [37], [38], [39], [40].

III. MATERIALS AND METHOD

A. STUDY AREA

This study focuses on two study sites located in Fiji, an island archipelago which sits in the Southwestern Pacific Ocean. It lies approximately between 15° to 20° South latitudes and between 175° and 182° East longitude.

The main islands are Viti Levu and Vanua Levu while the remaining islands are smaller, low-lying, and widely spread across the ocean [41]. Fiji experiences a mostly tropical climate with two major seasons observed annually – a warm and wet season from November to April, and a cool and dry season from May to October. The most significant influence on the rainy season is the South Pacific Convergence Zone causing the formation of tropical low-pressure systems and cyclones as well [42]. Additionally, there are localized and regional effects which impact the weather across the islands. One cause of this is the geography of the islands, particularly the two main islands of Viti Levu and Vanua Levu, which are of volcanic origins and generally have mountainous interior terrain with flatter coastal plains [43]. Another factor which affects localized weather on the major islands is the prevailing Southeast Trade Winds which cause greater cloud formation and precipitation on the eastern parts of the main islands.

TABLE 1. **The geographic description of the present study sites.**

Site Name	Location		
	Longitude (°E)	Latitude (°S)	Elevation (m)
Nadi International Airport	177.43	17.75	18
Nausori International Airport	178.55	18.03	5

The two sites are Nadi International Airport and Nausori International Airport, which are located on the main island of Viti Levu (Table 1). Nadi International Airport (Nadi) is the main international airport of the country and is located on the western side of the island, while Nausori International Airport (Nausori) is the secondary international airport and is located on the eastern part of the island. As the tourism industry is one of the largest revenue earners for the country, the airport and aviation efficiency and safety are imperative. These two airports are the locations where the meteorological observations are recorded on-site. These observations are routine aviation meteorological observations and are made following the international standards for aviation weather observations [44].

Since these two airports operate 24 hours a day, they are required by the International Civil Aviation Organization (ICAO) standards to provide these routine weather observations at the airport every hour for use by aviation stakeholders such as airlines and air traffic service providers. These reports are called METAR and contain meteorological parameters which have been specified by the World Meteorological Organization (WMO) to be observed and made available at airports. Although all meteorological parameters play a role in overall flight operations, the two target variables to be forecasted, i.e. visibility and ceiling are vital for safe and efficient flight operations during the crucial phases of landing and taking off.

B. DATASET

Historical meteorological data spanning over 10 years was used for the development of the proposed forecasting model. Table 2 (a) describes the variables in the dataset that were obtained for the development of the proposed forecasting model. The data was recorded from January 1st, 2012, 0000 local time to December 31st, 2021, 2300 local time. This equated to 87672 data instances with 12 variables which were recorded in numerical values.

The visibility variable was measured in kilometers, while the Total Low Cloud variable from the dataset was used as the ceiling. Total Low Cloud is measured in oktas and is the amount of low cloud covering the sky in eight parts. Even though instrument measurements are possible, current observations for these two variables are done manually following the standards set out by the WMO [44].

While preprocessing the data, the following data imputation methods were applied to fill in the missing values. Where there was a single missing value, a simple average of the preceding and succeeding values was taken. For instances of consecutive missing values, a combination of calendar-averaged values and simple averages was applied [45]. Additionally, flawed values (falling out of the range of correct values) were replaced with the median value for better model learning [46]. In terms of the missing values for visibility (Tabel 2 (b)), there were none for Nadi but around 13.5% of missing data was recorded for Nausori. Similarly, for total low cloud cover, Nadi has significantly fewer missing data (~3.6%) compared to Nausori with 23.26%. In respect to missing data, it was noticed that significant portions of the data were missing at Nausori. This could have been due to the station being unmanned for periods of time and no observations taken as the instances of missing data coincided with the lockdown during the Covid-19 pandemic. Thus, after analyzing data by year, the years with greater than 10% missing values were excluded from model building, which left 6 consecutive years of data for study site Nausori International Airport with total data of 52632 data points.

Table 2 (b) further gives statistical aggregates of the two predictor variables - visibility and total low cloud cover - for

TABLE 2. **The characteristics of the predictor and objective variables *used to develop the proposed hybrid IIS-LSTM integrated model for 1*-hourly visibility and total low cloud cover forecasting; and (b) the descriptive statistics of Visibility (km) and Total Low Cloud cover (oktas) with details of missing data.**

(a) Variable name	Units	Mode of measurement	Variable Type in Model
Air Temperature	°C	Instrument	Predictor Variable
Wet Bulb Temperature	°C	Instrument	Predictor Variable
Dew Point Temperature	°C	Instrument/ Calculated	Predictor Variable
Relative Humidity	%	Instrument/ Calculated	Predictor Variable
Rainfall	mm	Instrument	Predictor Variable
Mean Sea Level Pressure	hPa	Instrument	Predictor Variable
Wind Speed	m/s	Instrument	Predictor Variable
Wind Direction	°	Instrument	Predictor Variable
Total Cloud	Oktas	Manual observation	Predictor Variable
Total Low Cloud Height	m	Manual observation	Predictor Variable
Visibility	km	Manual observation	Objective Variable
Total Low Cloud	Oktas	Manual observation	Objective Variable

(b) Objective Variable	Station	Missing data (%)	Maximum	Minimum	Mean	Median	Skewness	Kurtosis
Visibility (km)	Nadi International Airport	0.02	50	0.10	46.19	50	-3.10	10.54
	Nausori International Airport	13.49	50	0.05	41.14	40	-1.70	2.31
Total Low Cloud cover (oktas)	Nadi International Airport	3.60	8	0	3.45	3	0.37	-0.69
	Nausori International Airport	23.26	8	0	5.28	6	-0.49	-0.86

the 2 study sites. The visibility magnitudes ranged from a maximum value of 50 km for both study sites to a minimum of 0.1 km at Nadi and 0.05 km at Nausori. The mean visibility was 46.19 km at Nadi, higher than the value at Nausori, which was 41.14 km.

The median visibility value was also higher at Nadi at 50 km compared to Nausori at 40 km. Furthermore, the visibility data at Nadi showed high negative skewness (−3.10) and leptokurtic (10.54) tendency compared to Nausori, which exhibited a similar tendency although to a lesser degree (Skewness=−1.70, Kurtosis=2.31). This indicated that much of the data distribution is greater than the mean values with a higher probability of it being on the tail end of the data distribution [47].

Considering the statistical aggregates for total low cloud cover, it was noticed that the range was from a maximum value of 8 to a minimum value of 0 oktas for both study sites. The mean and median scores are significantly different for the 2 study sites, with Nadi having 3.45 and 3 oktas, respectively, and Nausori having 5.28 and 6 oktas, respectively. This was consistent with the physical attributes at these two study sites, where Nausori is situated in a more cloudy and rainy part of the main island compared to Nadi. The skewness and kurtosis values of total low cloud cover at both study sites indicated an almost normal distribution.

C. PROPOSED MODEL DESIGN

1) DATA PRE-PROCESSING

After pre-processing the data, extraction of significant lagged inputs was carried out using cross-correlation (CCF) and partial auto-correlation function (PACF) statistical assessments. This assessment was also used to determine whether the target variables visibility and total low cloud cover have correlations both in time-space, as well as between other meteorological

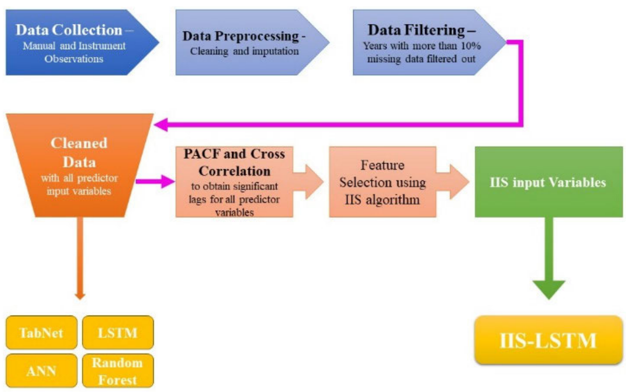

FIGURE 2. **Flowchart detailing the proposed methodology for the proposed hybrid IIS-LSTM model in the model development stage implemented forecast 1-hourly atmospheric visibility and total low cloud cover ceiling.**

variables. PACF and CCF were undertaken for both visibility and total low cloud cover target variables for the two study sites. Figure 3 shows the result of the CCF statistical assessments, which indicated the correlation of the target variable visibility or total low cloud cover with the predictor variables.

Meteorological variables in the dataset are stochastic and impacts are short-lived in nature, so only up to 24 antecedent lags are considered as longer lags would be unreliable in capturing useful information for predicting the target [48]. Similarly, Figure 4 shows the results of the PACF statistical assessment, which indicates the best preceding lagged values correlating to the target variable's value in that instance. Only lags up to 12 hours were considered due to the reason mentioned earlier. For both CCF and PACF, lags were considered significant if they exceeded the 95% confidence band. This generated a global pool of 151 features each for visibility and total low cloud cover at study site Nadi, and 154 features

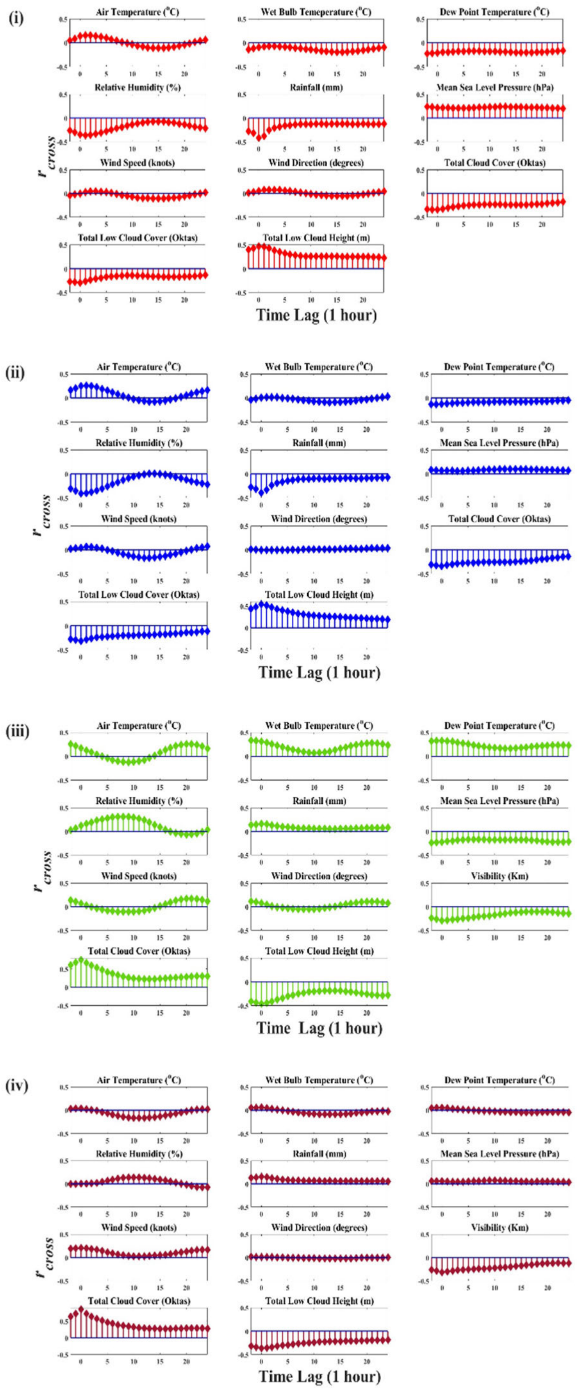

FIGURE 3. Cross-correlations coefficients (r_{cross}) showing the amount of co-variance between visibility vs. its predictor variables for the case of (i) Nadi and (ii) Nausori; and the co-variance between total low cloud *vs.* its predictor variables for the case of (iii) Nadi and (iv) Nausori.

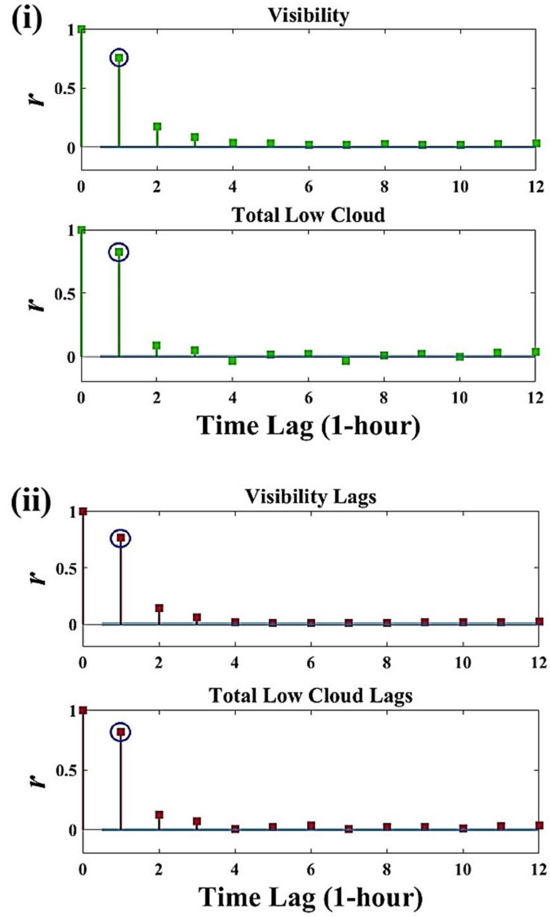

FIGURE 4. Partial Auto-Correlation Function (PACF) coefficient of the target variables for (i) Nadi and (ii) Nausori. The lag circled in blue indicates the most significant lagged inputs used in the development of the forecasting model.

each for study site Nausori. All predictor variables and their significant lags formed a matrix of global predictors.

2) THE IIS PROCEDURE

The global predictors were analyzed with the IIS algorithm of the proposed hybrid integrated model to extract the most useful features from this global list of features. Figure 5 illustrates the results for the two target variables at the two study sites from the IIS process. The cumulative performance of the Extra-Tree model within the IIS algorithm is R^2 denoted as the line graph in the plot while the contribution of each screened variable is ΔR^2, denoted by the bars on the plot. For Nadi's visibility target, the performance increased up to the second variable with the second hourly-lagged input of visibility being the most significant one. For target total low cloud cover, the performance of the model again increased up to the second variable with the first hourly lagged input of total low cloud being the most significant feature.

In contrast, for Nausori's target variable visibility, the performance increased up to the fourth variable; however, only 3 features were significant with the first lagged input of hourly rainfall being the most significant. For total low cloud cover, the performance of the model decreased after the second feature, with the first and fifth hourly lagged inputs of total low cloud cover being almost equally significant. It is noteworthy that the algorithm determined the optimum number of variables up to the point where additional variables decreased performance (as was the case in Figure 5(a) targets

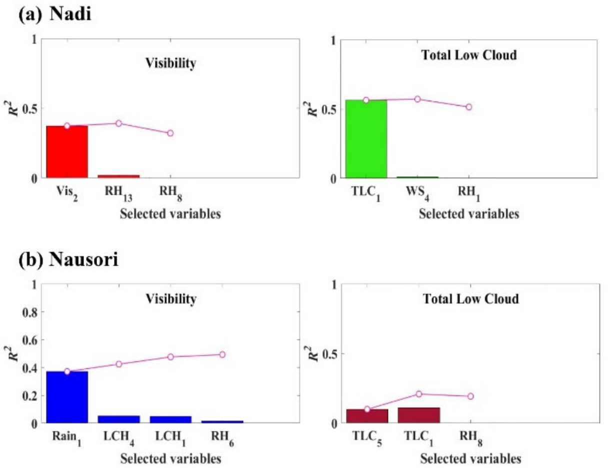

FIGURE 5. Cross-correlations coefficients (r_{cross}) showing the amount of co-variance between visibility vs. its predictor variables for the case of (i) Nadi and (ii) Nausori; and the co-variance between total low cloud *vs.* its predictor variables for the case of (iii) Nadi and (iv) Nausori.

visibility and total low cloud cover, and Figure 5(b) target total low cloud cover), or when an algorithm tolerance value, ε, of performance increase was not surpassed (as was the case in Figure 5(b) target visibility). Further insights into these results will be discussed in a later section.

3) THE PROPOSED IIS-LSTM MODELLING APPROACH

The IIS algorithm supplied the optimum dataset to be used in the chosen deep-learning LSTM forecasting model. This dataset was divided into a training and testing set with 20% of the training set used in validation to fine-tune the model [49]. Researchers have used different ratios of training set, such as 70% [31], [50] or 80% [51] as there are no set rules for dividing data [42]. Thus, in this study, the dataset had training (75%) and testing (25%) subsets.

The LSTM architecture was designed with one LSTM cell layer with 80 neurons, the sigmoid activation function, and a dense layer with a single output. This architecture was used to learn from the training subset data and make forecasts from the testing subset data after the data was reshaped into a format that could be acceptably processed by the model. The model was trained on different combinations of hyperparameters manually to achieve the optimum set of hyperparameters [51]. These were:

- optimizer = "adam"
- batch size = 15
- maximum epochs = 500
- Validation loss criteria = mae (Mean Absolute Error)

Furthermore, to prevent the model from overfitting or underfitting the data, early stopping [52] and ReduceLROn-Plateau [53] were utilized respectively. The early stopping method was employed in 10 epochs (patience=10) when there was no further decrease in the validation loss criteria and the lowest value was saved. ReduceLROnPlateau callback method reduced the learning rate when no improvement was detected with patience of 5 [49]. The simple design of the architecture was sufficient to achieve optimal model configuration as the number of features had been greatly reduced by the preceding IIS algorithm. This negated the need for an unnecessarily large architecture which reduced the training time of the model, and the generalization of data for improved predictions [54].

4) MODEL EVALUATION PROCEDURE

The superiority of the proposed hybrid IIS-LSTM integrated model was tested by forecasting using the predictor variable from the testing subset and evaluating it with the observed data.

The performance evaluation metrics included Pearson's Correlation Coefficient (r), Willmott's Index (WI), Nash-Sutcliffe Efficiency Index (E_{NS}), Root Mean Squared Error ($RMSE$), Mean Absolute Error (MAE), Legate-McCabe Efficiency Index (LM) and Kling-Gupta Efficiency Index (KGE) [55], [56], [57], [58], [59]. These evaluation metrics are widely used in research and their mathematical equations are as follows:

Pearson's Correlation Coefficient (r)

$$r = \frac{n\left(\Sigma y\hat{y}\right) - \left(\Sigma y\right)\left(\Sigma \hat{y}\right)}{\sqrt{\left[n\Sigma y^2 - (\Sigma y)^2\right]\left[n\Sigma \hat{y}^2 - \left(\Sigma \hat{y}\right)^2\right]}} \quad (-1 \leq \text{r} \leq 1) \tag{1}$$

Willmott's Index (WI)

$$WI = 1 - \frac{\Sigma_{i=1}^{N}\left[y - \hat{y}\right]^2}{\Sigma_{i=1}^{N}\left[\left|\hat{y} - \bar{y}\right| + \left|y - \bar{y}\right|\right]^2} \quad (0 \leq WI \leq 1) \tag{2}$$

Nash Sutcliffe's Coefficient (E_{NS})

$$E_{NS} = 1 - \left[\frac{\Sigma_{i=1}^{N}\left(y - \hat{y}\right)^2}{\Sigma_{i=1}^{N}\left(y - \bar{y}\right)^2}\right] \quad (-\infty \leq E_{NS} \leq 1) \tag{3}$$

Root Mean Squared Error ($RMSE$)

$$RMSE\left(y, \hat{y}\right) = \sqrt{\frac{1}{n}\sum\nolimits_{0}^{n-1}\left(y_i - \hat{y}_i\right)^2} \tag{4}$$

Mean Absolute Error (MAE)

$$MAE\left(y, \hat{y}\right) = \frac{1}{n}\sum\nolimits_{0}^{n-1}\left|y_i - \hat{y}_i\right| \tag{5}$$

Legate and McCabe's Index (LM)

$$LM = 1 - \left[\frac{\Sigma_{i=1}^{N}\left|y - \hat{y}\right|}{\Sigma_{i=1}^{N}\left|y - \bar{y}\right|}\right] \quad (-\infty \leq LM \leq 1) \tag{6}$$

Kling-Gupta Efficiency (KGE)

$$KGE = 1 - \sqrt{(r-1)^2 + \left(\frac{\hat{y}}{y} - 1\right)^2 + \left(\frac{C\hat{V}}{CV}\right)^2} \quad (-\infty \leq KGE \leq 1) \tag{7}$$

In the equations above, the observed value for the target variable's visibility and total low cloud cover is represented as y, while the predicted value from the model is denoted $\hat{y}$ from the model. The metrics for our objective model were then compared with metrics output by the benchmark models.

The benchmark models included standalone Artificial Neural Networks (ANN) [60], Random Forest [61], the deep learning LSTM [62], and TabNet [63] models. These models were selected due to their optimal forecasting performance using atmospheric and meteorological data as shown in previous work [31], [37], [64], [65].

IV. RESULTS

This section presents the outcomes of the performance evaluation of the proposed hybrid IIS-LSTM integrated model with competition models for forecasting hourly visibility and hourly total low cloud cover using meteorological data as model inputs. The competing models included standalone TabNet, LSTM, ANN, and RF. The predictive performance of the proposed hybrid IIS-LSTM integrated model was tested against these benchmark models for the two study sites at a 1-hour forecasting horizon. The performances are summarized using the evaluation metrics as in (1) – (7) and assessed via graphical means.

Table 3 shows the outcomes of all the performance metrics for each model design for the two sites. From the results, *the* proposed hybrid IIS-LSTM integrated model produced the best outputs based on the performance evaluation metrics used.

For Nadi, the IIS-LSTM model has the highest agreement indices (r ≈ 0.73, WI ≈ 0.83, E_{NS} ≈ 0.52) and the lowest error metrics (RMSE ≈ 4.81 km, MAE ≈ 1.9 km) for visibility forecasts. It also registered the highest agreement indices (r ≈ 0.84, WI ≈ 0.91, E_{NS} ≈ 0.71) and least values of error (RMSE ≈ 0.92 oktas, MAE ≈ 0.67 oktas) for total low cloud forecasts.

Likewise, for Nausori, the IIS-LSTM model produced the highest agreement indices ($r \approx 0.72$, $WI \approx 0.82$, $E_{NS} \approx 0.52$) and least error (RMSE ≈ 8.08 km, MAE ≈ 5.1 km) for visibility forecast. Similarly, it has the highest agreement indices ($r \approx 0.78$, $WI \approx 0.87$, $E_{NS} \approx 0.60$) and lowest error values error ($RMSE \approx 1.23$ oktas, $MAE \approx 0.93$ oktas) for total low cloud forecasts (Table 3).

A widely used evaluation metric to measure agreement between predicted and observed values is the Nash-Sutcliffe Index (E_{NS}). This is a dimensionless value and is a scaled version of the mean squared error. However, a limitation of this index is that it can exaggerate the impact of extreme outliers. To address this, Willmott's Index (*WI*) is used because it considers the ratio of the mean squared error instead of the differences [66]. This testing performance is considered one of the most robust parameters to evaluate the superiority of a model against its competitors [50].

Figure 6 shows a 3D bar graph portraying the *WI* for each model. In Figure 6(i), for the case of visibility forecasting, the improvement in the model's performance can be seen with the proposed hybrid IIS-LSTM integrated model compared to the benchmark models. The IIS-LSTM model had

TABLE 3. The testing performance of the proposed hybrid IIS-LSTM integrated model compared with the standalone models using all variables. (a) Objective variable 1: Visibility for (i) Nadi International Airport and (ii) Nausori International Airport, and (b) Objective variable 2: Total Low Cloud for (i) Nadi International Airport and (ii) Nausori International Airport. Note: r = Pearson's Correlation coefficient, WI = Willmott's Index, E_{NS} = Nash Sutcliffe Efficiency coefficient, $RMSE$ = root mean square error, and MAE = mean absolute error. The most accurate model is boldfaced, presented in orange.

(a) Visibility	Predictive Models	r	WI	E_{NS}	$RMSE$ (km)	MAE (km)
(i) Nadi	**IIS-LSTM**	**0.7273**	**0.8282**	**0.5207**	**4.8107**	**1.8963**
	TABNet	0.0563	0.3186	-0.6312	8.9395	7.5721
	LSTM	0.0186	0.2658	-0.2461	7.7568	6.0288
	Random Forest	0.0508	0.1244	-40.311	44.9871	44.4478
	ANN	0.0203	0.1244	-40.297	44.9794	44.4397
(ii) Nausori	**IIS-LSTM**	**0.7214**	**0.8207**	**0.5199**	**8.0807**	**5.1022**
	TABNet	0.6438	0.7670	0.3122	9.7433	7.2442
	LSTM	0.5813	0.6954	0.2869	9.8477	7.7477
	Random Forest	0.6045	0.2938	-10.584	39.9857	38.2955
	ANN	0.5999	0.2942	-10.542	39.9144	38.2224

(b) Total Low Cloud	Predictive Models	r	WI	E_{NS}	$RMSE$ (km)	MAE (km)
(i) Nadi	**IIS-LSTM**	**0.8403**	**0.9071**	**0.7057**	**0.9249**	**0.6723**
	TABNet	0.8140	0.8850	0.6564	0.9915	0.7359
	LSTM	0.7875	0.8705	0.6146	1.0585	0.8248
	Random Forest	0.7902	0.5181	-1.3386	2.5869	2.1727
	ANN	0.7945	0.5122	-1.476	2.6618	2.254
(ii) Nausori	**IIS-LSTM**	**0.7785**	**0.8674**	**0.6043**	**1.2283**	**0.9297**
	TABNet	0.7288	0.8344	0.5190	1.3599	1.0733
	LSTM	0.7003	0.8086	0.4851	1.4012	1.1349
	Random Forest	0.7195	0.4457	-3.2828	4.0578	3.6609
	ANN	0.677	0.4443	-3.2448	4.0398	3.6315

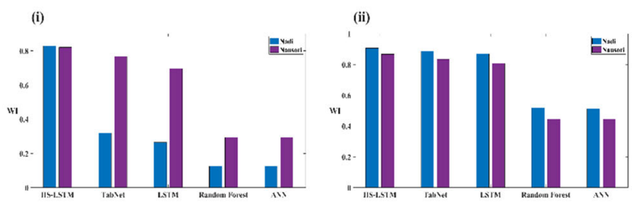

FIGURE 6. Testing performance of IIS-LSTM vs. the 4 competing models evaluated using the Willmott index of agreement (WI) for (i) visibility and (ii) total low cloud.

approximately 0.83 score for Nadi and 0.82 score for Nausori, which was an increase of almost 160% from the second-best performing model for Nadi and an increase of 7% for Nausori.

Similarly, Figure 6(ii) depicts the *WI* performance for total low cloud cover forecasts. Again, the IIS-LSTM models have the best score at site Nadi with approximately 0.91 and Nausori with 0.87 which is an approximate increase of 2.5% and 4 % respectively. The proposed hybrid IIS-LSTM integrated model produces the best agreement between the observed and predicted outputs compared to the benchmark models in our dataset.

Comparatively, Figure 7 shows the error metrics used to evaluate the model performances, where Root Mean Squared Error (*RMSE*) is used. For visibility forecasts (Figure 7(i)) the proposed hybrid IIS-LSTM integrated model produces the lowest error for Nadi with 4.81 km and 8.08 km for Nausori. When comparing the error for total low cloud forecasts (Figure 7(ii)) the IIS-LSTM model again has the lowest value of *RMSE* at approximately 0.92 oktas for Nadi and 1.23 oktas for Nausori. Based on these results, the proposed hybrid IIS-LSTM integrated model has been shown to minimize the *RMSE* for the forecast at both study sites with this dataset.

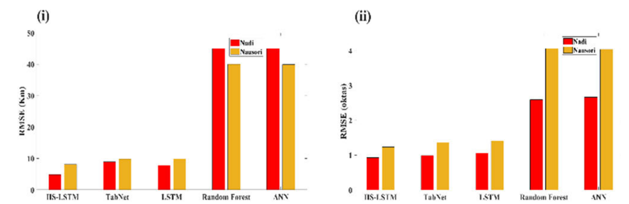

FIGURE 7. 3D Bar graph of root mean square error in the testing phase of the IIS-LSTM vs. the 4 competing models for (i) visibility *(RMSE, km)* and for (ii) total low cloud *(RMSE, oktas)*.

TABLE 4. Evaluating the Testing performance of the proposed hybrid IIS-LSTM integrated model for one-hourly forecasts for (a) Objective variable 1: Visibility for (i) Nadi International Airport and (ii) Nausori International Airport, and (b) Objective variable 2: Total Low Cloud for (i) Nadi International Airport and (ii) Nausori International Airport; using *LM* = Legate's and McCabe's Index, and *KGE* = Kling-Gupta efficiency. The best model is boldfaced and presented in orange.

(a) Visibility	Predictive Models	*LM*	*KGE*
(i) Nadi	**IIS-LSTM**	**0.3972**	**0.6447**
	TABNet	-1.3406	-0.1883
	LSTM	-0.9165	-0.3868
	Random Forest	-12.739	-0.6532
	ANN	-12.737	-0.6758
(ii) Nausori	**IIS-LSTM**	**0.4046**	**0.5954**
	TABNet	0.1558	0.5844
	LSTM	0.0959	0.4141
	Random Forest	-3.4627	-0.389
	ANN	-3.4542	-0.3886

(b) Total Low Cloud	Predictive Models	*LM*	*KGE*
(i) Nadi	**IIS-LSTM**	**0.5382**	**0.7621**
	TABNet	0.4876	0.7131
	LSTM	0.4335	0.6959
	Random Forest	-0.5127	-0.0178
	ANN	-0.5693	-0.0339
(ii) Nausori	**IIS-LSTM**	**0.4404**	**0.6833**
	TABNet	0.3587	0.6407
	LSTM	0.3169	0.5772
	Random Forest	-1.1872	-0.1226
	ANN	-1.1697	-0.1363

The Legates and McCabe's Index *(LM)* is an improved measure from the *WI* which further eliminates the amplification from outliers by removing the squaring effect [56].

Compatibly, the *KGE* avoids the limitations of the E_{NS} by computing the Euclidian distance of the correlation, bias, and variability measure instead of it being scaled by the standard deviation of the observed values [67]. Table 4 shows these alternative metrics used to evaluate the model's performance, *LM* and *KGE*. For visibility forecasts, the proposed hybrid IIS-LSTM integrated model has the highest value of *LM* with 0.397 and 0.405 for Nadi and Nausori respectively.

Likewise, for total low cloud cover forecasts, the IIS-LSTM model scores were 0.538 and 0.440 for Nadi and Nausori respectively. Negative values for some benchmark models can be *attributed to* the lower bound of this coefficient being negative infinity, indicating poor performance of these models [68].

When the *KGE* metrics are considered, the proposed hybrid IIS-LSTM integrated model performed the best according to this criterion as well. When considering visibility forecasts, the Nadi and Nausori international airport site scores of 0.645 and 0.595 were registered by the IIS-LSTM model respectively. Similarly, for total low cloud cover forecasts, the IIS-LSTM model had the highest scores of 0.762 and 0.683 for Nadi and Nausori airports, respectively.

V. DISCUSSION

In this section, the results of this study are expounded on in terms of its highlights as well as its limitations of the present study. The proposed hybrid IIS-LSTM integrated model has shown its superiority in performance compared to the benchmark models in forecasting visibility and total low cloud cover at two study sites. This was shown from the results of various performance evaluation metrics depicted in the previous section.

The results emphasized the suitability of the IIS algorithm in selecting useful features for the model. This is consistent with the outcomes of similar studies, such as [30], where the results from the performance metrics (*WI*, E_{NS}, *RMSE* and *MAE*) determined the suitability of the IIS-optimized model compared to the standalone models. As previously deduced by [28], IIS was a useful tool for selecting non-redundant inputs in different test conditions (e.g., different sites, different target variables, presence of several redundant features). Removal of redundant features was shown to be an important aspect affecting the forecasting accuracy of data-driven models. Fewer input variables imply low dimensionality of the sources of uncertainty and lower propagation of error from input variables [33].

Additionally, the LSTM model's efficiency in 'learning' and making predictions from this time-series data is also pivotal in this study. Reference [13] concluded from their results that ML methods can improve the visibility and ceiling forecasts up to an hour ahead forecast horizon when accurate observations are used for analysis.

Similarly, [15] recommended the development of deep learning models, particularly LSTM models, from their study due to LSTM's ability to extract time-dependent features from the raw data auto automatically and its increase in efficiency when the size of the training set increases.

Referring to the results of the features selected by the IIS algorithm as shown in Figure 5, some assumptions can be made regarding the correlation between the objective variable and the optimal feature selected variables. For visibility forecasting, the most significant feature at Nadi International Airport was the second lagged value of visibility, while for Nausori international airport it was the first lagged value of the Rainfall variable. The difference in the selected feature can be explained by the geography of the sites, as Nausori International Airport is located in the region which receives significantly more rainfall, while Nadi International Airport is located in the drier region of the country.

The study of [64] reported that for December 2023, Nadi airport received 57.7 mm of rainfall while Nausori airport received 181 mm of rainfall. The total days of rainfall were

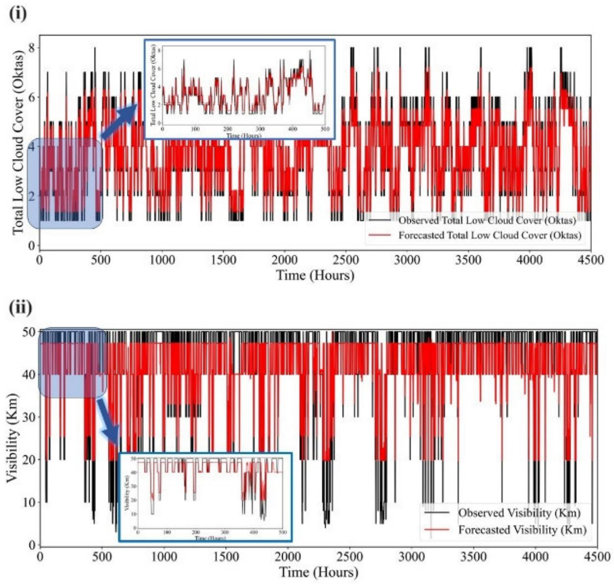

FIGURE 8. 3D Comparison of observed (actual) and forecasted (predicted) values for the IIS-LSTM model in the testing phase for (i) Visibility – Nausori, and (ii) Total Low Cloud – Nadi.

11 for Nadi airport and 21 for Nausori airport, which is 28% and 68% of the month respectively and represents a difference of 40% rain days a month between the two sites. Rainfall is naturally known to be a significant physical factor in the reduction of visibility [70], [71].

Consequently, variation in rainfall data was the most important factor in determining the variation in visibility at Nausori International Airport than it was for Nadi International Airport. On the other hand, when the optimal variable for total low cloud cover is considered at both study sites, the most significant feature variable is the 1st hourly lagged data series of total low cloud cover, with Nausori also having the 5th hourly lagged data series as equally significant.

Clouds have been difficult to forecast due to their 3D nature, various physical properties such as coverage, thickness, top height and base height, and the different types of clouds. Additionally, mechanisms driving cloud formation vary from region to region and current models offer mesoscale resolution in cloud forecasts and extrapolation for higher resolution forecasts [72], [73]. Therefore, it is reasonable that the IIS algorithm identified the lagged values of only total low cloud cover as the optimal and reliable features for future total low cloud cover predictions.

Generalization of the model was an important factor for consideration with the design of the proposed hybrid IIS-LSTM integrated model, ensuring that the model's applicability is not limited to the study locations used for this research. This was achieved firstly by training the model on a large dataset which accounted for variations caused by daily and seasonal changes. Secondly, the IIS component ensured that the model learned patterns of data from only the relevant features affecting the predictand. It also reduced dimensionality and complexity of the model, preventing overfitting on the data used for this study. Additionally, early stopping technique and an overall simple architecture of the LSTM algorithm contributed to the prevention of overfitting.

Figure 8 takes a closer look at the comparison between the observed data and the forecasted output. When Figure 8(i) is examined visually, the visibility graph of the forecasted output follows the pattern of the graph of the observed outputs for Nadi. However, the values at the lower extremities are not fairly forecasted. A possible reason for this could be a limitation in the dataset.

As noted in Table 2 (b) earlier, the visibility data for Nadi has a mean of 46.19 km, a median of 50 km, and notably, a high kurtosis of −3.10. This indicated that many of the data points in the higher extremity and the lower values are not proportionately represented in the dataset. This would have been a factor when the model was trained as the extreme magnitudes might not have been properly captured.

Added to this fact is the consistency and accuracy of the observational data. For instance, visibility data is collected through manual observations according to international aviation meteorological observation standards at both study sites. The data intervals vary, ranging from 50m intervals when visibility is less than 800m; 100m intervals until 5 km; 1 km intervals until 10 km; and 10 km intervals until 50 km [44]. Thus, manual observations could readily be affected by irregularities from different observers and would not have been as consistent as instrument measurements adding another layer of complexity.

VI. CONCLUSION

In this study, a hybrid deep learning IIS-LSTM integrated model is proposed for forecasting visibility and total low cloud cover for two study sites in Fiji, Nadi International Airport and Nausori International Airport. The proposed model was tested against four benchmark models using performance evaluation metrics for a 1-hourly forecast horizon.

The following are the main contributions and key findings of this research:

1. The analysis focusing on hourly aviation meteorological observation data for Nadi International Airport and Nausori International Airport found key statistical metrics of target variables visibility and total low cloud cover to develop models.

2. A hybrid IIS-LSTM integrated model was presented which combined the effectiveness of the IIS algorithm to select the optimum features from the range of predictor variables and their significant lags, with the deep learning LSTM model with the superior capability for time-series forecasting.

3. The robustness of the proposed hybrid IIS-LSTM integrated model to forecast visibility and total low cloud cover was illustrated when the performance of the IIS-LSTM model was evaluated against the benchmark models (TabNet, LSTM, ANN, RF). The objective model had the highest agreement metrics (r, WI, ENS) while also having the least error (RMSE, MAE) compared to the benchmark models.

4. This research study makes a significant contribution to knowledge in the scope of visibility forecasts as a regression problem using deep learning models, and a first of any kind of AI-based forecasting study of visibility and total low cloud cover predictions for the chosen study sites.

5. The development of this objective model using only hourly aviation meteorological observation data indicates the capacity of this method to be extended to any station with similar data for further investigative research into practical usage in the aviation industry.

The approach undertaken for this study can be enhanced with the scope of further research. Firstly, model hyperparameters for this study were optimized with an inexhaustive grid search method. This can be improved with state-of-the-art techniques such as Hyperband [74] and Bayesian Optimization [75], [76], which can further assist in fine-tuning the model to attain the optimum architecture of the model and its forecast. Additionally, the potential for data inconsistency which could have arisen from manual measurements of the visibility and low cloud cover variables in the data can be mitigated through the use of instrument measures. Moreover, recording and using shorter and near-real-time data would be beneficial bearing in mind the highly dynamic nature of visibility and cloud base, since current industry and ICAO standards have meteorological data being collected at hourly intervals.

Further independent study can be undertaken to evaluate forecasts at higher timesteps, such as 3-hour, 6-hour, 12-hour or 24-hour horizons as necessary for practical operational use. The approach undertaken in this study can be extended to other aviation meteorological data collection sites in Fiji and elsewhere. This will verify the applicability of this approach beyond the study sites, as well as the possibilities of connecting multiple sites in a network for higher resolution forecasts for a region.

The main factor in implementing the proposed forecasting model effectively is data availability and data quality. In order to have high quality data for aviation purposes, the main prerequisite is that the data needs to be recorded under the ICAO standards. The recording station needs to be certified by both the International Civil Aviation Organization (ICAO) and the World Meteorological Organization (WMO). The data for this study was obtained from the Fiji Meteorological Service which abide by WMO and ICAO standards for aviation meteorological reports. The observations are made according to international requirements, which ensures that data is consistent, accurate, reliable, and reported in standardized units. Such weather reports, which are readily available for specific locations, would be reliable for use in the proposed model. Additional factors would need to be addressed to have the proposed model's practical implementation for operational use. Firstly, the model would need to be modified accordingly to accept real-time data and produce real-time analysis. Secondly, comparisons to assess the accuracy and reliability of this proposed hybrid model with existing forecasting tools in a live environment will have to be undertaken. Thirdly, the appropriate computational resources will need to be allocated based on whether a cloud based, or in-situ model is implemented. For example, an online cloud-based system would not be suitable for remote and maritime locations with poor or no internet connectivity. Hence, in-situ models would need to be parsimonious (as shown by the removal of the redundant features using IIS) and lightweight requiring least computational resources. Other considerations include assessing the practicality of use for the proposed model as a forecasting tool at a particular location considering the availability of other such tools.

Looking further towards the adoption and acceptance of the proposed model as a predictive tool used within the aviation industry, important considerations must be taken into account. The aviation industry is a highly regulated industry, especially for aviation stakeholders operating under the International Civil Aviation Organization body, and any change to standard operating procedures are assessed subject to very standards before being adopted for widespread use. However, such predictive tools still have a niche such as in general aviation, private or recreational flights. It could be used by pilots flying to destinations with a limited flight information service provision but having weather reports available at or in the vicinity of the airport. Additionally, it could be a cost-effective but efficient tool for flight information service providers at airports where there is a lack of infrastructure for accurate on-site forecasts, such as at remote or private airports. Therefore, this study paves the path for further applications of AI in aviation industry, particularly forecasting of important parameters such as visibility and cloud base.

ACKNOWLEDGMENT

The first author is a recipient of Australian Awards Scholarship from Australian Federal Government and is therefore grateful to the Department of Foreign Affairs and Trade for funding this study through Australian Awards scholarship scheme from 2022 to 2024. Disclaimer: The views and opinions expressed in this article are those of the authors and do not represent the views of the Australian Government. The authors thank Fiji Meteorological Services for providing routine aviation meteorological observation data required for this project.

REFERENCES

[1] *Annex 3 to the Convention on International Civil Aviation: Meteorological Service for International Air Navigation*, Int. Civil Aviation Org. (ICAO), Montreal, QC, Canada, 2004.

[2] *Annex 2 to the Convention on International Civil Aviation: Rules of the Air*, Int. Civil Aviation Org. (ICAO), Montreal, QC, Canada, 2005.

[3] P. Herzegh, G. Wiener, R. Bateman, J. Cowie, and J. Black, "Data fusion enables better recognition of ceiling and visibility hazards in aviation," *Bull. Amer. Meteorol. Soc.*, vol. 96, no. 4, pp. 526–532, Apr. 2015.

[4] A. J. Fultz and W. S. Ashley, "Fatal weather-related general aviation accidents in the United States," *Phys. Geography*, vol. 37, no. 5, pp. 291–312, Sep. 2016.

[5] K. R. Fenton Jr., D. M. Mueller, T. R. Peevey, M. S. Wandishin, and M. A. Petty, *Ceiling and Visibility Analysis Products Assessment*, document OAR GSD-64, NOAA Tech. Memorandum, Office Ocean. Atmos. Res., Nat. Ocean. Atmos. Admin., 1972.

[6] D. P. Solomatine and A. Ostfeld, "Data-driven modelling: Some past experiences and new approaches," *J. Hydroinformatics*, vol. 10, no. 1, pp. 3–22, Jan. 2008.

[7] L. C. Ortega, L. D. Otero, C. E. Otero, and A. Fabregas, "Visibility forecasting with deep learning," in *Proc. IEEE Int. Syst. Conf. (SysCon)*, Aug. 2020, pp. 1–7.

[8] K. Wang, H. Zhao, A. Liu, and Z. Bai, "The risk neural network based visibility forecast," in *Proc. 5th Int. Conf. Natural Comput.*, vol. 1, Aug. 2009, pp. 338–341.

[9] L. Zhu, G. Zhu, L. Han, and N. Wang, "The application of deep learning in airport visibility forecast," *Atmos. Climate Sci.*, vol. 7, no. 3, pp. 314–322, 2017.

[10] D. Guijo-Rubio, P. A. Gutiérrez, C. Casanova-Mateo, J. Sanz-Justo, S. Salcedo-Sanz, and C. Hervás-Martínez, "Prediction of low-visibility events due to fog using ordinal classification," *Atmos. Res.*, vol. 214, pp. 64–73, Dec. 2018.

[11] S. Cornejo-Bueno, D. Casillas-Pérez, L. Cornejo-Bueno, M. I. Chidean, A. J. Caamaño, J. Sanz-Justo, C. Casanova-Mateo, and S. Salcedo-Sanz, "Persistence analysis and prediction of low-visibility events at Valladolid airport, Spain," *Symmetry*, vol. 12, no. 6, p. 1045, Jun. 2020.

[12] L. Ortega, L. D. Otero, and C. Otero, "Application of machine learning algorithms for visibility classification," in *Proc. IEEE Int. Syst. Conf. (SysCon)*, Apr. 2019, pp. 1–5, doi: 10.1109/SYSCON.2019.8836910.

[13] F. M. Cordeiro, G. B. França, F. L. de Albuquerque Neto, and I. Gultepe, "Visibility and ceiling nowcasting using artificial intelligence techniques for aviation applications," *Atmosphere*, vol. 12, no. 12, p. 1657, Dec. 2021.

[14] C. Castillo-Botón, D. Casillas-Pérez, C. Casanova-Mateo, S. Ghimire, E. Cerro-Prada, P. A. Gutierrez, R. C. Deo, and S. Salcedo-Sanz, "Machine learning regression and classification methods for fog events prediction," *Atmos. Res.*, vol. 272, Jul. 2022, Art. no. 106157.

[15] L. C. Ortega, L. D. Otero, M. Solomon, C. E. Otero, and A. Fabregas, "Deep learning models for visibility forecasting using climatological data," *Int. J. Forecasting*, vol. 39, no. 2, pp. 992–1004, Apr. 2023, doi: 10.1016/j.ijforecast.2022.03.009.

[16] C. Peláez-Rodríguez, J. Pérez-Aracil, A. de Lopez-Diz, C. Casanova-Mateo, D. Fister, S. Jiménez-Fernández, and S. Salcedo-Sanz, "Deep learning ensembles for accurate fog-related low-visibility events forecasting," *Neurocomputing*, vol. 549, Sep. 2023, Art. no. 126435, doi: 10.1016/j.neucom.2023.126435.

[17] F. Curreri, S. Graziani, and M. G. Xibilia, "Input selection methods for data-driven soft sensors design: Application to an industrial process," *Inf. Sci.*, vol. 537, pp. 1–17, Oct. 2020, doi: 10.1016/j.ins.2020.05.028.

[18] F. A. A. Souza, R. Araújo, and J. Mendes, "Review of soft sensor methods for regression applications," *Chemometric Intell. Lab. Syst.*, vol. 152, pp. 69–79, Mar. 2016, doi: 10.1016/j.chemolab.2015.12.011.

[19] P. Y. Chen and P. M. Popovich, *Correlation: Parametric and Nonparametric Measures*, vol. 139. Newbury Park, CA, USA: Sage, 2002.

[20] M. G. Kendall, *Rank Correlation Methods*. London, U.K.: Charles Griffin, 1948.

[21] G. J. Székely, M. L. Rizzo, and N. K. Bakirov, "Measuring and testing dependence by correlation of distances," *Ann. Statist.*, vol. 35, no. 6, pp. 2769–2794, Dec. 2007, doi: 10.1214/009053607000000505.

[22] D. V. Sridhar, E. B. Bartlett, and R. C. Seagrave, "Information theoretic subset selection for neural network models," *Comput. Chem. Eng.*, vol. 22, nos. 4–5, pp. 613–626, Jan. 1998, doi: 10.1016/s0098-1354(97)00227-5.

[23] E. K. Onyari and F. M. Ilunga, "Application of MLP neural network and M5P model tree in predicting streamflow: A case study of Luvuvhu catchment, South Africa," *Int. J. Innov., Manage. Technol.*, vol. 4, no. 1, pp. 11–15, 2013.

[24] M. Radovic, M. Ghalwash, N. Filipovic, and Z. Obradovic, "Minimum redundancy maximum relevance feature selection approach for temporal gene expression data," *BMC Bioinf.*, vol. 18, no. 1, p. 9, Dec. 2017, doi: 10.1186/s12859-016-1423-9.

[25] X. He and H. Asada, "A new method for identifying orders of input–output models for nonlinear dynamic systems," in *Proc. Amer. Control Conf.*, Jun. 1993, pp. 2520–2523, doi: 10.23919/ACC.1993.4793346.

[26] K. Sun, S.-H. Huang, D. S. Wong, and S.-S. Jang, "Design and application of a variable selection method for multilayer perceptron neural network with LASSO," *IEEE Trans. Neural Netw. Learn. Syst.*, vol. 28, no. 6, pp. 1386–1396, Jun. 2017, doi: 10.1109/TNNLS.2016.2542866.

[27] M. M. Rahman, S. A. Imtiaz, and K. Hawboldt, "A hybrid input variable selection method for building soft sensor from correlated process variables," *Chemometric Intell. Lab. Syst.*, vol. 157, pp. 67–77, Oct. 2016, doi: 10.1016/j.chemolab.2016.06.015.

[28] M. Han, R. Zhang, and M. Xu, "Multivariate chaotic time series prediction based on ELM-PLSR and hybrid variable selection algorithm," *Neural Process. Lett.*, vol. 46, no. 2, pp. 705–717, Oct. 2017, doi: 10.1007/s11063-017-9616-4.

[29] S. Galelli and A. Castelletti, "Tree-based iterative input variable selection for hydrological modeling," *Water Resour. Res.*, vol. 49, no. 7, pp. 4295–4310, Jul. 2013, doi: 10.1002/wrcr.20339.

[30] S. Galelli, G. B. Humphrey, H. R. Maier, A. Castelletti, G. C. Dandy, and M. S. Gibbs, "An evaluation framework for input variable selection algorithms for environmental data-driven models," *Environ. Model. Softw.*, vol. 62, pp. 33–51, Dec. 2014, doi: 10.1016/j.envsoft.2014.08.015.

[31] R. Prasad, R. C. Deo, Y. Li, and T. Maraseni, "Input selection and performance optimization of ANN-based streamflow forecasts in the drought-prone Murray darling basin region using IIS and MODWT algorithm," *Atmos. Res.*, vol. 197, pp. 42–63, Nov. 2017, doi: 10.1016/j.atmosres.2017.06.014.

[32] P. Geurts, D. Ernst, and L. Wehenkel, "Extremely randomized trees," *Mach. Learn.*, vol. 63, no. 1, pp. 3–42, Apr. 2006, doi: 10.1007/s10994-006-6226-1.

[33] L. Mejía and M. Barrios, "Identifying watershed predictors of surface water quality through iterative input selection," *Int. J. Environ. Sci. Technol.*, vol. 20, no. 7, pp. 7201–7216, Jul. 2023, doi: 10.1007/s13762-022-04406-2.

[34] S. Ghimire, R. C. Deo, D. Casillas-Pérez, and S. Salcedo-Sanz, "Efficient daily electricity demand prediction with hybrid deep-learning multi-algorithm approach," *Energy Convers. Manage.*, vol. 297, Dec. 2023, Art. no. 117707, doi: 10.1016/j.enconman.2023.117707.

[35] Y. Lin, Y. Yan, J. Xu, Y. Liao, and F. Ma, "Forecasting stock index price using the CEEMDAN-LSTM model," *North Amer. J. Econ. Finance*, vol. 57, Jul. 2021, Art. no. 101421, doi: 10.1016/j.najef.2021.101421.

[36] Y. Yu, X. Si, C. Hu, and J. Zhang, "A review of recurrent neural networks: LSTM cells and network architectures," *Neural Comput.*, vol. 31, no. 7, pp. 1235–1270, Jul. 2019, doi: 10.1162/neco_a_01199.

[37] E. Sharma, R. C. Deo, R. Prasad, A. V. Parisi, and N. Raj, "Deep air quality forecasts: Suspended particulate matter modeling with convolutional neural and long short-term memory networks," *IEEE Access*, vol. 8, pp. 209503–209516, 2020, doi: 10.1109/ACCESS.2020.3039002.

[38] E. Sharma, R. C. Deo, J. Soar, R. Prasad, A. V. Parisi, and N. Raj, "Novel hybrid deep learning model for satellite based PM10 forecasting in the most polluted Australian hotspots," *Atmos. Environ.*, vol. 279, Jun. 2022, Art. no. 119111, doi: 10.1016/j.atmosenv.2022.119111.

[39] Le, Ho, Lee, and Jung, "Application of long short-term memory (LSTM) neural network for flood forecasting," *Water*, vol. 11, no. 7, p. 1387, Jul. 2019, doi: 10.3390/w11071387.

[40] R. C. Staudemeyer and E. Rothstein Morris, "Understanding LSTM—A tutorial into long short-term memory recurrent neural networks," 2019, *arXiv:1909.09586*.

[41] J. T. Berdach, *Republic of the Fiji Islands: Country Environmental Analysis. Mainstreaming Environmental Considerations in Economic and Development Planning Processes*, document TA:6039-REG, Asian Develop. Bank, Mandaluyong, Philippines, 2005.

[42] Australian Bureau of Meteorology and CSIRO. (2011). *Climate Change in the Pacific: Scientific Assessment and New Research*. [Online]. Available: https://www.pacificclimatechangescience.org/wp-content/uploads/2013/09/Volume-2-country-reports.pdf

[43] Fiji Meteorological Service. (2006). *The Climate of Fiji*. [Online]. Available: https://www.met.gov.fj/ClimateofFiji.pdf

[44] *Technical Regulations Basic Documents No. 2*, 2021st ed., vol. 2, World Meteorological Org., Geneva, Switzerland, 2018.

[45] R. C. Deo, X. Wen, and F. Qi, "A wavelet-coupled support vector machine model for forecasting global incident solar radiation using limited meteorological dataset," *Appl. Energy*, vol. 168, pp. 568–593, Apr. 2016, doi: 10.1016/j.apenergy.2016.01.130.

[46] L. P. Joseph, R. C. Deo, D. Casillas-Pérez, R. Prasad, N. Raj, and S. Salcedo-Sanz, "Short-term wind speed forecasting using an optimized three-phase convolutional neural network fused with bidirectional long short-term memory network model," *Appl. Energy*, vol. 359, Apr. 2024, Art. no. 122624, doi: 10.1016/j.apenergy.2024.122624.

[47] R. Bono, J. Arnau, R. Alarcón, and M. J. Blanca, "Bias, precision, and accuracy of skewness and kurtosis estimators for frequently used continuous distributions," *Symmetry*, vol. 12, no. 1, p. 19, Dec. 2019, doi: 10.3390/sym12010019.
[48] L. P. Joseph, R. C. Deo, R. Prasad, S. Salcedo-Sanz, N. Raj, and J. Soar, "Near real-time wind speed forecast model with bidirectional LSTM networks," *Renew. Energy*, vol. 204, pp. 39–58, Mar. 2023, doi: 10.1016/j.renene.2022.12.123.
[49] S. Ghimire, R. C. Deo, D. Casillas-Pérez, and S. Salcedo-Sanz, "Electricity demand error corrections with attention bi-directional neural networks," *Energy*, vol. 291, Mar. 2024, Art. no. 129938, doi: 10.1016/j.energy.2023.129938.
[50] E. Sharma, R. C. Deo, R. Prasad, and A. V. Parisi, "A hybrid air quality early-warning framework: An hourly forecasting model with online sequential extreme learning machines and empirical mode decomposition algorithms," *Sci. Total Environ.*, vol. 709, Mar. 2020, Art. no. 135934.
[51] M. Moishin, R. C. Deo, R. Prasad, N. Raj, and S. Abdulla, "Designing deep-based learning flood forecast model with ConvLSTM hybrid algorithm," *IEEE Access*, vol. 9, pp. 50982–50993, 2021.
[52] Jahandad, S. M. Sam, K. Kamardin, N. N. A. Sjarif, and N. Mohamed, "Offline signature verification using deep learning convolutional neural network (CNN) architectures GoogLeNet Inception-v1 and Inception-v3," *Proc. Comput. Sci.*, vol. 161, pp. 475–483, Jan. 2019, doi: 10.1016/j.procs.2019.11.147.
[53] F. Zhou, Z. Huang, and C. Zhang, "Carbon price forecasting based on CEEMDAN and LSTM," *Appl. Energy*, vol. 311, Apr. 2022, Art. no. 118601, doi: 10.1016/j.apenergy.2022.118601.
[54] N. Karunanithi, W. J. Grenney, D. Whitley, and K. Bovee, "Neural networks for river flow prediction," *J. Comput. Civil Eng.*, vol. 8, no. 2, pp. 201–220, Apr. 1994, doi: 10.1061/(asce)0887-3801(1994)8:2(201).
[55] H. V. Gupta and H. Kling, "On typical range, sensitivity, and normalization of mean squared error and Nash–Sutcliffe efficiency type metrics," *Water Resour. Res.*, vol. 47, no. 10, pp. 1–3, Oct. 2011, doi: 10.1029/2011WR010962.
[56] D. R. Legates and G. J. McCabe, "Evaluating the use of 'goodness-of-fit' measures in hydrologic and hydroclimatic model validation," *Water Resour. Res.*, vol. 35, no. 1, pp. 233–241, Jan. 1999, doi: 10.1029/1998wr900018.
[57] J. E. Nash and J. V. Sutcliffe, "River flow forecasting through conceptual models Part I—A discussion of principles," *J. Hydrol.*, vol. 10, no. 3, pp. 282–290, Apr. 1970, doi: 10.1016/0022-1694(70)90255-6.
[58] C. J. Willmott, "On the validation of models," *Phys. Geography*, vol. 2, no. 2, pp. 184–194, Jul. 1981, doi: 10.1080/02723646.1981.10642213.
[59] C. J. Willmott, "On the evaluation of model performance in physical geography," in *Spatial Statistics and Models*. Dordrecht, The Netherlands: Springer, 1984, pp. 443–460, doi: 10.1007/978-94-017-3048-8_23.
[60] T.-W. Kim and J. B. Valdés, "Nonlinear model for drought forecasting based on a conjunction of wavelet transforms and neural networks," *J. Hydrologic Eng.*, vol. 8, no. 6, pp. 319–328, Nov. 2003, doi: 10.1061/(asce)1084-0699(2003)8:6(319).
[61] L. Breiman, "Random forests," *Mach. Learn.*, vol. 45, no. 1, pp. 5–32, 2001, doi: 10.1023/A:1010933404324.
[62] S. Hochreiter and J. Schmidhuber, "Long short-term memory," *Neural Comput.*, vol. 9, no. 8, pp. 1735–1780, Nov. 1997, doi: 10.1162/neco.1997.9.8.1735.
[63] S. Ö. Arik and T. Pfister, "TabNet: Attentive interpretable tabular learning," in *Proc. AAAI Conf. Artif. Intell.*, 2021, pp. 6679–6687.
[64] Y. Zhang, X. Yao, Q. Wu, Y. Huang, Z. Zhou, J. Yang, and X. Liu, "Turbidity prediction of lake-type raw water using random forest model based on meteorological data: A case study of Tai lake, China," *J. Environ. Manage.*, vol. 290, Jul. 2021, Art. no. 112657, doi: 10.1016/j.jenvman.2021.112657.
[65] J. Yan, T. Xu, Y. Yu, and H. Xu, "Rainfall forecast model based on the TabNet model," *Water*, vol. 13, no. 9, p. 1272, Apr. 2021, doi: 10.3390/w13091272.
[66] S. Ghimire, R. C. Deo, D. Casillas-Pérez, and S. Salcedo-Sanz, "Two-step deep learning framework with error compensation technique for short-term, half-hourly electricity price forecasting," *Appl. Energy*, vol. 353, Jan. 2024, Art. no. 122059, doi: 10.1016/j.apenergy.2023.122059.
[67] H. V. Gupta, H. Kling, K. K. Yilmaz, and G. F. Martinez, "Decomposition of the mean squared error and NSE performance criteria: Implications for improving hydrological modelling," *J. Hydrol.*, vol. 377, nos. 1–2, pp. 80–91, Oct. 2009, doi: 10.1016/j.jhydrol.2009.08.003.
[68] D. R. Legates and G. J. McCabe, "A refined index of model performance: A rejoinder," *Int. J. Climatol.*, vol. 33, no. 4, pp. 1053–1056, Mar. 2013, doi: 10.1002/joc.3487.
[69] *Fiji Climate Summary December 2023*, Fiji Meteorological Service, Nadi Airport Nadi, Fiji, Jan. 2024.
[70] F. Bernardin, R. Bremond, V. Ledoux, M. Pinto, S. Lemonnier, V. Cavallo, and M. Colomb, "Measuring the effect of the rainfall on the windshield in terms of visual performance," *Accident Anal. Prevention*, vol. 63, pp. 83–88, Feb. 2014, doi: 10.1016/j.aap.2013.10.008.
[71] S. Wang, T. Chen, B. Yu, Y. Sun, and X. Qin, "Coupling impacts of spray and rainfall on road visibility and vehicle speeds: A simulation-based analysis," *Can. J. Civil Eng.*, vol. 49, no. 7, pp. 1220–1230, Jul. 2022, doi: 10.1139/cjce-2021-0402.
[72] C. Nguyen et al., "Machine learning-based cloud forecast corrections for fusions of numerical weather prediction model and satellite data," *Artif. Intell. for Earth Syst.*, vol. 2, no. 3, pp. 1–21, Jul. 2023, doi: 10.1175/aies-d-22-0072.1.
[73] Q.-Z. Ye and S.-S. Chen, "The ultimate meteorological question from observational astronomers: How good is the cloud cover forecast?" *Monthly Notices Roy. Astronomical Soc.*, vol. 428, no. 4, pp. 3288–3294, Feb. 2013, doi: 10.1093/mnras/sts278.
[74] L. Li, K. Jamieson, G. DeSalvo, A. Rostamizadeh, and A. Talwalkar, "Hyperband: A novel bandit-based approach to hyperparameter optimization," *J. Mach. Learn. Res.*, vol. 18, pp. 1–52, Apr. 2018.
[75] J. Wang, J. Xu, and X. Wang, "Combination of hyperband and Bayesian optimization for hyperparameter optimization in deep learning," 2018, *arXiv:1801.01596*.
[76] K. Eggensperger, M. Feurer, F. Hutter, J. Bergstra, J. Snoek, H. Hoos, and K. Leyton-Brown, "Towards an empirical foundation for assessing Bayesian optimization of hyperparameters," in *Proc. NIPS Workshop Bayesian Optim. Theory Practice*, vol. 10, no. 3, 2013, pp. 1–5.

SHIVEEL RAJ received the bachelor's degree in science from the University of Fiji, in 2015. He is currently pursuing the Master of Research degree with the UniSQ's Advanced Data Analytics Laboratory, School of Mathematics, Physics and Computing, University of Southern Queensland, Australia. His research interests include visibility forecasting, artificial intelligence, and machine learning.

RAVINESH C. DEO (Senior Member, IEEE) received the B.Sc. degree (Hons.) from the University of the South Pacific, Fiji, the M.Sc. degree from the University of Canterbury, New Zealand, and the Ph.D. degree in signal processing from The University of Adelaide. He leads the UniSQ's Advanced Data Analytics Laboratory, University of Southern Queensland, Australia. He was recognized as a Clarivate Highly Cited Researcher (1 in 2,828 researchers for research performance) in Top 1% among scientists with demonstrated influence. He mentored more than 40 higher degree students, many receiving a best thesis award. He received an Excellence in Research Award and the Ronel Erwee Memorial Award for Excellence in Postgraduate Supervision and Faculty Research Excellence, University and School Publication, Faculty Teaching Excellence and Elsevier Highly Cited Papers for impactful contributions. He has secured significant grants and has published more than 300 articles with cumulative citations of more than 15,000 and a H-index of 71.

EKTA SHARMA is currently an Artificial Intelligence (AI) Researcher funded by the Office of National Intelligence, Australian Government. She works on solving space challenges through AI and also a Research Fellow for Women with the STEMM Discipline, University of Southern Queensland. She has received an Excellence Award for her Ph.D. degree in AI and a commendation from the Deputy High Commissioner of Australian High Commission to India, in 2022, for her innovative research on early warning systems for bushfires. She has authored seven books and has a strong technical background in Asia, Switzerland, and Australia. Her qualifications in operations research and mathematics have earned her numerous grants and competitive funding for women working in big data. She is the recent Winner of the Women in Technology Award and a Finalist for the Queensland Women in STEM. Her research interests include space-based situational awareness, satellite communications, and environmental challenges.

RAMENDRA PRASAD received the B.Sc. degree in mathematics and in physics and the M.Sc. degree in physics from the University of the South Pacific, Fiji, and the Ph.D. degree in modeling and simulations from the University of Southern Queensland, Australia, in 2019. Currently, he is a Senior Lecturer with The University of Fiji. He has authored/coauthored 40 articles in peer-reviewed journals and reputed conferences. His research interests include modeling and simulations, advanced machine learning approaches, advanced data analytics, hydrological modeling, energy modeling, energy management, environmental and atmospheric modeling, and ocean wave modeling.

TOAN DINH is currently an Associate Professor with the School of Engineering, University of Southern Queensland, Australia. His research interests include micro and nano-electromechanical systems (MEMS/NEMS), semiconductor physics, sensors for harsh environments, advanced materials for health monitoring, and the application of machine learning in engineering applications.

SANCHO SALCEDO-SANZ was born in Madrid, Spain, in 1974. He received the B.S. degree in physics from the Universidad Complutense de Madrid, Spain, in 1998, the Ph.D. degree in telecommunications engineering from the Universidad Carlos III de Madrid, Spain, in 2002, and the Ph.D. degree in physics from the Universidad Complutense de Madrid, in 2019. He spent one year with the School of Computer Science, The University of Birmingham, U.K., as a Postdoctoral Research Fellow. Currently, he is a Full Professor with the Department of Signal Processing and Communications, Universidad de Alcalá, Spain. He has coauthored more than 220 international journal articles in the field of machine learning and soft-computing and its applications. His current research interests include soft-computing techniques, hybrid algorithms, and neural networks in different problems of science and technology.